

Rheological and tribological properties of ZrP intercalation compounds as lubricating grease thickener

Yiling Wu

Taiyuan University of Technology

Zhiguo Hou

Taiyuan University of Technology

Xinrui Zhao

Taiyuan University of Technology

Jinxiang Dong

dongjinxiangwork@hotmail.com

Taiyuan University of Technology

Hong Xu

Taiyuan University of Technology

Research Article

Keywords: ZrP intercalation compounds, Grease thickeners, Rheology, Tribological properties

Posted Date: January 8th, 2024

DOI: <https://doi.org/10.21203/rs.3.rs-3831604/v1>

License:  This work is licensed under a Creative Commons Attribution 4.0 International License.

[Read Full License](#)

Additional Declarations: No competing interests reported.

Version of Record: A version of this preprint was published at Tribology Transactions on April 24th, 2024.

See the published version at <https://doi.org/10.1080/10402004.2024.2345724>.

Abstract

Here, we study layered zirconium phosphate intercalated with octadecyltrimethylammonium bromide (STAB-ZrP) as a thickener by thickening five types of base oils. The layered structure and morphology of STAB-ZrP after thickening were confirmed by X-ray diffraction (XRD) and scanning electron microscopy (SEM). The thickening ability and fluidity behavior of STAB-ZrP gel were evaluated using rheological measurements. The tribological properties of STAB-ZrP gel were investigated using a reciprocating tribometer under temperatures of 25°C and -15°C. The rheological results showed that STAB-ZrP gel had grease-like characteristics. Naphthenic and alkyl naphthalene as the base oil can lead to the higher thickening ability. Naphthenic oil maintained the most colloidal stability at 25°C and -15°C. STAB-ZrP gel exhibited superior anti-wear and friction reduction, owing to the formation of a solid protective film on the contact interface. This research established the relationship of STAB-ZrP with base oils in terms of their performance. STAB-ZrP acts as both a thickener and a solid additive in the STAB-ZrP gel system. This study can serve a beneficial trial for future preparations of lubricating grease.

1 Introduction

Friction causes extensive mechanical wear and power loss, such that one-fifth of total global energy consumption stems from friction and wear [1]. Synthetic lubricants are widely utilized in moving machine parts, metal cutting, power transmission, and so on. Lubricating grease is one of most important lubricants. Due to its anti-wear, anti-friction, corrosion resistance, and sealing properties, lubrication grease is widely used in bearings, gears, and other lubrication areas [2]. Among the many types of lubricating grease, lithium grease is currently the most applicable grease, owing to its excellent performance [3], but with the rapid development of the lithium battery industry, the soaring price of lithium restricts the sustainable development of lithium-based grease. As such, there is an urgent need to develop new types of thickeners.

Lubricating grease is a semi-fluid product derived from thickening agents in base oils. That is, thickening agents with well-arranged structural forms are sufficiently dispersed in a base oil [4]. The basic components of lubricating grease are base oils, thickeners, and additives. Thickeners have an extremely important role in the grease system because they hold the base oil and the additives together. They form the skeleton of the grease. Lithium grease with metal lithium soap as a thickener has a chemical structure of long-chain fatty acid lithium salt, which is composed of an alkyl chain carboxylic acid anion with lithium cation. To make lithium soap, 12-hydroxystearic acid is reacted with lithium hydroxide to form long-chain fatty acid lithium salts, and these lithium salts form soap fibers by self-assembly in the base oil [3].

Recently, when studying of the lubricating properties of layered zirconium phosphate, our group found that octadecyltrimethylammonium bromide intercalated zirconium phosphate (STAB-ZrP) had a soap structure similar to metal lithium soap. In the STAB-ZrP layered structure, layered planes are constituted of zirconium octahedra ZrO_6 and monohydrogen phosphate tetrahedral groups (HPO_4). The interlayer

region is occupied by octadecyltrimethylammonium ions and links the layered plane via the protonated P–O groups. So the layered structure of STAB-ZrP is just like lithium soap. The key difference is that lithium soap is derived from self-assembly, and a chemical reaction is needed to prepare the soap preparation (a chemically neutralized soap). By contrast, STAB-ZrP is pre-assembled. The gel preparation only needs STAB-ZrP to be widely distributed in the base oil to form colloid suspension.

Base oils are the largest components of lubricating greases, accounting for 80.0–97.0 wt.% [5, 6]. They are categorized as mineral oils (naphthenic and paraffinic oils), synthetic hydrocarbons (polyalphaolefins (PAO) and alkylates), other synthetic compounds (esters and polyglycols), and so on. The nature of the base oil has an important impact on the physicochemical and tribological behavior of the grease. Yaroslav et al. [7] studied the effects of eight types of oils: mineral oils S-9, MS-8, and AU; hydrogenated oils GK, NB3020, and VHVI-4 oils; and polyalphaolefin oils PAO-2 and PAO-4 on the thickening and lubricating properties of lithium soap. They found that the content of hydrocarbon types (paraffin-based, cycloalkyl, and aromatic) affected the viscosity and anti-wear properties of the greases. As the aromatic content of the base oil increases, the viscosity of the base oil increased and the anti-wear properties deteriorated. The grease prepared using PAO-4 had minimal change in viscosity with temperature, and displayed optimal low-temperature lubricating properties. Nan Xu et al. [8] synthesized a series of lithium greases with different thickener concentrations by using PAO, PAO complexed with alkylated naphthalene, and PAO complexed with ester oils as the base oils. The results showed that the introduction of base oils with molecular chains (containing ester bonds and aryl rings) significantly increased the structural strength of the lithium grease. Enhui Zhang et al. [9] prepared four types of lithium-based greases with paraffin oil, naphthenic oil, PAO oil and polyol ester oil as base oils. The results showed that the naphthenic oil-based grease had the best colloidal stability, and the PE-based grease had the worst colloidal stability. The PE-based grease had the best recoverability but the lowest structural strength. Laurentis N D et al. [10] studied the lubricating properties of lithium soap with mineral oil, PAO, and a blend of PAO and ester oil. They found that friction was affected by the nature of the base oil. Specifically, the friction of the grease using PAO as the base oil was lower than that of mineral oil on the same oil viscosity.

Taken together, the literature indicates that the base oil has an important influence on both the thickening and lubricating properties of grease. Herein, we consider STAB-ZrP as a new thickener. We selected five types of oils to study the thickening ability and lubricating performance of STAB-ZrP gel: paraffin-based mineral oil (S8), cycloalkyl mineral oil (KN4010), polyalphaolefin synthetic oil (PAO8), alkyl naphthalene synthetic oil Synesstic 5 (AN), and pentaerythritol ester synthetic oil Esterex NP451 (POE). STAB-ZrP was used as the thickener to prepare STAB-ZrP oleogels. After the thickening process, the layered structure and morphology of STAB-ZrP powder were analyzed to study changes to the interlayer spacing and aggregation state of STAB-ZrP particles. Subsequently, the rheological behavior of the obtained STAB-ZrP gels was investigated using a rheometer to evaluate the thickening ability of the five types of oils. Finally, we evaluated the friction and wear performance of STAB-ZrP gels using an SRV tribometer in reciprocating mode. Their contact surfaces lubricated by STAB-ZrP gels were analyzed

after friction tests to ascertain the element composition of the tribofilms. On the basis of the results, we uncovered the relationship of STAB-ZrP to the type of base oil in terms of their performance.

2 Experiment

2.1 Materials

Table 1
Basic properties of the five types of base oils

Base oil type	Mineral oil		Synthetic oil		
	Paraffin (S8)	Naphthenic (KN4010)	Poly- α -olefin (PAO)	alkyl naphthalene (AN)	Pentaerythritol ester(POE)
Kinematic viscosity at 40°C(mm ² /s)	43.40	172	48.0	29.0	25
Kinematic viscosity at 100°C(mm ² /s)	6.35	11.62	8.0	4.7	5
Viscosity index	127	22	139	74	130
Pour point(°C)	-15	-30	-48	-39	-60

Phosphoric acid (H₃PO₄), octadecyl trimethyl ammonium bromide (STAB), and zirconium oxychloride octahydrate (ZrOCl₂·8H₂O) were purchased from Aladdin (Shanghai) Reagent Co., Ltd. Ethyl acetate and petroleum ether were purchased from Tianjin Kemiou Reagent Co., Ltd. None of the reagents was purified. Paraffin-based mineral oil S8 was purchased from Korea Shuanglong Oil Chemical Industry Ltd. KN4010 naphthenic mineral oil was purchased from PetroChina Karamay Petrochemical Company. Poly- α -olefin synthetic oil SpectraSyn8 (PAO-8), alkyl naphthalene synthetic oil Synesstic 5 (AN), and pentaerythritol ester synthetic oil Esterex NP451 (POE) were purchased from ExxonMobil Corporation. The typical physical and chemical properties of the five base oils are shown in Table 1.

2.2 Sample preparation

2.2.1 STAB-ZrP preparation

According to the amount calculated, water (H₂O), phosphoric acid (H₃PO₄), zirconium oxychloride octahydrate (ZrOCl₂·8H₂O), and octadecyl trimethyl ammonium bromide (STAB) were added into a Teflon-lined stainless steel reactor in order. After mixing these fully, the steel reactor lid was firmly shut and the reactor was placed into an oven at constant temperature. Then, it was laid out for natural cooling after reaching the crystallization time.

2.2.2 Preparation of STAB-ZrP gel

The prepared STAB-ZrP sample was washed using hot water, and a white precipitate was collected by centrifugation. The precipitate and ethyl acetate were added to a beaker, stirred at room temperature for 30 min, and then centrifuged. The centrifuged STAB-ZrP was mixed with the base oil and stirred for 3 h. Then, the STAB-ZrP oil mixture was aged in an oven at 150°C for 5 h. After cooling down to room temperature, the obtained STAB-ZrP gel was homogenized three times in a triple-roller mill.

2.3 Test methods

2.3.1 Powder sample characterization

The raw STAB-ZrP powder was used directly for analysis. The STAB-ZrP gel samples with different base oils needed to be washed with petroleum ether to remove the oil. They were centrifuged and dried in an oven at 100°C. The crystal structure of all STAB-ZrP samples was characterized using an Ultima IV X-ray diffractometer (PXRD, CuK α , $\lambda = 1.5418 \text{ \AA}$, 40 kV, 40 mA). The scanning speed was 0.5°/min. The microscopic morphology of the STAB-ZrP powder samples was observed using a Hitachi SU8010 Scanning Electron Microscope with an operating voltage of 3 kV. Infrared spectra were recorded on an IRAffinity-1 infrared spectrometer using compacted KBr pellets. Thermogravimetric analysis was carried out with a Setaram Instruments Labsystems EVO Simultaneous Thermal Analyzer in air atmosphere at a rate of 5°C/min.

2.3.2 Characterization of physical and chemical properties of STAB-ZrP gels

To investigate the effect of STAB-ZrP thickener content on the rheological properties of STAB-ZrP gel samples with different base oils, the rheological properties of the STAB-ZrP gel samples were measured using a rheometer (MCR 302, Anton Paar) equipped with a plate-to-plate sandblasted parallel disk (25 mm diameter, 1 mm gap). The variation of elastic modulus G' and loss modulus G'' with shear stress τ was investigated in oscillatory mode at a frequency of 1 Hz and strain amplitude $\gamma = 0.01\text{--}100.0\%$. The effect of temperature on the viscoelastic properties of 10.0 wt.% STAB-ZrP gel samples with different base oils was measured at -15°C and 25°C. The apparent viscosity of the base oils and STAB-ZrP gels was also measured at -15°C and 25°C under a shear rate of 1 s^{-1} .

We used the ASTM D 6184-17 grease steel-mesh oil separation test to analyze oil separation in the STAB-ZrP gel samples. The GB/T 3498 – 2008 grease dropping point test was used to determine the dropping point of STAB-ZrP gel samples. The test results are shown in Table 2.

2.3.3 Tribological test

The tribological properties of the STAB-ZrP gel samples were evaluated using an Optimal SRV-V Friction Wear Tester according to the ASTM D5707-14 standard test method. The reciprocating motion mode was in the form of point-to-point contact. The friction pair consisted of an upper sample steel ball and a lower sample steel disk. The steel ball was produced by Shanghai Steel Ball Factory: the material was GCr15, its diameter was 10 mm, and its Rockwell hardness was 59–64. The steel disk was produced by

Beijing Keli Yongcheng Science and Technology Development Co., Ltd., with a diameter of 24 mm and a Rockwell hardness of 59–61. Before the friction test, the ball and disk specimens were ultrasonically cleaned using petroleum ether. The SRV tester automatically output and recorded real-time dynamic friction coefficient curves. After the test, the amount of wear on the steel disk was observed with a Zegage-type three-dimensional white light interferometer from ZYGO, USA. The experiment was repeated three times under the same conditions.

3 Results and discussion

The powder samples before and after thickening STAB-ZrP were analyzed with an X-ray diffractometer (XRD). After the thickening process, all obtained STAB-ZrP samples maintained their original layered crystal structure (Fig. 1a). Except for the KN4010G gel sample, the first characteristic peak ($2\theta = 2.46^\circ$) of the STAB-ZrP gel samples with PAO, POE, AN, and S8 as base oils clearly shifted forward, and the corresponding interlayer spacing increased by 0.26 nm, 0.09 nm, 0.22 nm, and 0.03 nm, respectively. This experimental result indicated that part of the base oil had entered the STAB-ZrP interlayer (Fig. 1b).

Figures 2a–f show SEM photos of the STAB-ZrP samples before and after thickening. The pristine STAB-ZrP powder had an aggregated lamellar morphology (Fig. 2a). After the thickening process, the morphology of STAB-ZrP powder was no longer aggregated, forming cavities of different sizes (black circles). This phenomenon indicated that the base oil had stayed in the lamellae.

Figure 3 shows the thermogravimetric curves of the STAB-ZrP samples before and after the thickening process. From the thermogravimetric curves, it can be seen that there are three distinct stages of weight loss. The first stage occurred between 25°C and 180°C, corresponding to surface-adsorbed water and interlayer crystalline water. The second phase occurred between 180°C and 600°C and corresponded to the interlayer organic matter, which was 45.37 wt.%, 46.33 wt.%, 47.43 wt.%, 55.78 wt.%, 50.51 wt.%, and 50.93 wt.% for STAB-ZrP, S8G, KN4010G, PAOG, ANG, and POEG. After the thickening process, the weight loss of interlayer organic matter clearly increased. This is probably because some amount of base oil remained in the interlayer of STAB-ZrP. The third stage occurred between 600°C and 800°C and corresponded to the condensation process of P-OH, which finally produced ZrP_2O_7 [11].

3.1 Rheological behavior of STAB-ZrP gel with different base oils

Each type of base oil has its own chemical molecular structure, so the physical and chemical property of each type of oil is different (e.g., kinematic viscosity, pour point). As STAB-ZrP is a new type of thickening agent, the thickening ability STAB-ZrP with different types of base oils will be different.

Figures 4a–e show the viscoelastic curves of the STAB-ZrP gel samples with the five base oils under different STAB-ZrP content. It can be seen that the storage modulus (G') of all STAB-ZrP gel samples increased with increasing STAB-ZrP content. As the shear stress increased, the value of G' decreased

gradually, and the loss modulus (G'') value increased at the same time. The viscoelastic behavior of STAB-ZrP gel agreed with the viscoelastic characteristics of the grease reported in previous literature [8, 9, 12, 13]. The results indicated that STAB-ZrP as a thickener can thicken the five types of base oils.

To better compare the thickening ability of the five types of base oils, Fig. 4f demonstrates the relationship between the storage modulus of STAB-ZrP gel and STAB-ZrP content. When the STAB-ZrP content was under 7.5 wt.%, there was not much difference among the five base oils. As the STAB-ZrP content increased to 10.0 wt.%, the difference became increasingly clear. The G' value of S8G had no obvious increase with an increase in STAB-ZrP content. The G' value of POEG was gradually higher with increasing STAB-ZrP content. But the increasing degree of both S8G and POEG was clearly lower than that of PAOG, ANG, and KN4010G. The G' values for PAOG, ANG, and KN4010G all increased linearly as the STAB-ZrP content increased. When the STAB-ZrP content was at 15.0 wt.%, the storage modulus value of S8G, POEG, PAOG, KN4010G, and ANG was 22,357 Pa, 56,432 Pa, 138,740 Pa, 177,710 Pa, and 242,130 Pa, respectively. Thus, AN oil and KN4010 oil had the best thickening ability among the five types oil. Moreover, PAO oil was better than S8 oil and POE oil.

The reason for the superior performance of AN oil and KN4010 oil may originate from their chemical structure. Enhui Zhang et al. [9] reported that naphthenic oil-based lithium grease had the best colloidal stability among paraffin oil, naphthenic oil, polyalphaolefin oil, and polyol ester oil. Garshin et al. [14] investigated the thickening ability of eight oils on polyurethane grease. They found that an increase in the content of naphthenic and aromatic hydrocarbons in the base oil could increase the thickening ability of polyurea grease. In our STAB-ZrP gel study, alkyl naphthalene oil and cycloalkyl KN4010 oil also showed excellent thickening ability.

Since KN4010G and ANG were too viscous at 15.0 wt.% STAB-ZrP, the storage modulus value of 10.0 wt.% STAB-ZrP gel with the five oils all reached more than 5000 Pa, showing a good thickening effect. Thus, in subsequent experiments the STAB-ZrP content was set at 10.0 wt.%. Photographs of 10.0 wt.% STAB-ZrP gel samples with the five base oils are shown in Fig. 5 STAB-ZrP gel samples resembled lubricating grease in appearance, and had the same color as their base oils.

As STAB-ZrP gel is a non-Newtonian fluid, temperatures may affect the viscoelasticity and fluidity behavior of the gel. We chose two temperatures (25°C and -15°C) for further investigation.

Figure 6a compares the storage modulus value of STAB-ZrP gel with the five types of oils at temperatures of 25°C and -15°C. We found that the storage modulus of STAB-ZrP gel at -15°C was in all cases higher than that at 25°C. When the temperature dropped to -15°C, the storage modulus value of paraffin oil S8G, naphthenic oil KN4010G, polyolefin oil PAOG, alkylated naphthalene oil ANG and pentaerythritol ester oil POEG increased by 20.9, 2.9, 2.8, 3.8 and 4.5 times, respectively. S8G with paraffin oil as the base oil had the biggest increment. There were only subtle differences among the other four base oils.

Figure 6b shows the variation of flow index (τ_f/τ_y) of STAB-ZrP gel with the five oils at the temperatures of 25°C and -15°C. Here, τ_f is the shear stress corresponding to the flow point of the gel, and τ_y is the shear stress corresponding to the yield point of the gel. When τ_f/τ_y is equal to 1, the grease begins from a semi-solid state to a flow state and the internal gel structure becomes damaged [15]. At 25°C, the flow index of S8G, POEG, ANG, KN4010G and PAOG was 10.05, 9.45, 9.15, 12.67, and 5.69, respectively. When the temperature dropped to -15°C, the flow index of S8G, POEG, ANG, KN4010G, and PAOG was 1.54, 2.15, 6.23, 24.36, and 8.25, respectively. Thus, KN4010G had the highest flow index value among the five STAB-ZrP gel samples, indicating that KN4010 had very good thickening properties, especially under low temperature. Among the five STAB-ZrP gel samples, KN4010G always maintained the most stable gel structure at 25°C and -15°C. The flow index values of PAOG and ANG had small changes in amplitude. For S8G and POEG, the flow index values dramatically decreased at -15°C, indicating that the colloidal stability of S8G and POEG worsened at low temperature.

As 90 wt.% composition of STAB-ZrP gel is the base oil, the viscosity of the base oils can have an important effect on the fluidity of the gel [7, 16], especially at low temperatures [7]. Therefore, the apparent viscosities of the five types of base oils and their STAB-ZrP gels were investigated at 25°C and -15°C. The results are shown in Figs. 7a and 7b. It can be seen that the apparent viscosity trends of all STAB-ZrP gel samples were going in the same direction as their base oils, indicating that the apparent viscosity of STAB-ZrP gel depends on the viscosity of its base oil. The apparent viscosities of the five base oils and their STAB-ZrP gels increased as the temperature decreased.

The oil separation and dropping points of 10.0 wt.% STAB-ZrP gels with the five base oils are listed in Table 2. The dropping points of S8G, KN4010G, PAOG, ANG, and POEG were 322.5°C, 320.3°C, 295.0°C, 310.5°C, and 232.0°C, and the oil separation was 11.47 wt.%, 2.20 wt.%, 7.80 wt.%, 5.43 wt.%, and 15.37 wt.%, respectively. Among the five STAB-ZrP gels, KN4010G had the highest dropping point and lowest oil separation.

Table 2
Oil separation and dropping points of 10.0 wt.% STAB-ZrP gels with the five base oils

Gels	Dropping point / °C	Oil separation / wt.%
S8G	322.5	11.47
KN4010G	320.3	2.20
PAOG	293.0	7.80
ANG	310.5	5.43
POEG	232.0	15.37

3.2 Tribological properties of STAB-ZrP gel with different base oils

The wear volume and mean friction coefficients of the five base oils and their prepared STAB-ZrP gels are shown in Fig. 8. When the temperature was 25°C, the KN4010, AN, and POE base oils could run through the whole process, but not S8 and PAO. By contrast, all STAB-ZrP gel samples not only ran smoothly during the whole process, but also had much lower wear volume and mean friction coefficient values than their base oils. When the temperature decreased to -15°C, the PAO, AN, and POE base oils could finish the friction test, but not S8. In comparison, STAB-ZrP gel with S8, PAO, AN, and POE as base oils could go through the whole test, but with KN4010G, a seizure occurred due to high viscosity. Obviously, even at low temperatures, the STAB-ZrP gel samples had less wear volume and mean friction coefficient values than their base oils. The values of wear volume and mean friction coefficients of the STAB-ZrP gel samples at -15°C were slightly higher than at 25°C.

The wear surface morphology and elemental distribution of worn surfaces lubricated by the base oils and their STAB-ZrP gels were analyzed using 3D non-contact surface morphology (3D), scanning electron microscopy (SEM), and X-ray diffraction spectroscopy (EDS).

As shown in Fig. 9, at 25°C, the worn surfaces lubricated by STAB-ZrP gels were shallow and smooth. However, the worn surfaces of the five base oils were larger and covered with deep furrows. The SEM morphology was similar to the 3D images. For base oils, there were C, Fe, and Cr elements on the surfaces of the steel disks, which all belonged to the steel disk itself. The STAB-ZrP gels contained not only C, Fe, and Cr elements but also P and Zr elements on the worn surfaces, indicating that STAB-ZrP adheres to the surface to form a protective film.

Figure 10 shows analysis results at -15°C. Except for KN4010G, the wear surface state of all STAB-ZrP gels was obviously better than that of their base oils. The worn surfaces were also smaller and shallower than those of their base oils. But the worn surfaces had more scratches than at 25°C, and this result was consistent with the test results. Layered zirconium phosphate as a solid additive has been widely used in oils and greases to improve their anti-wear and anti-friction properties [17–21]. The friction results showed that STAB-ZrP is not only a thickener but also a good solid lubricant in the STAB-ZrP gel system.

From the above results, STAB-ZrP as a thickener can thicken the five types of base oils. During the thickening process, STAB-ZrP particles fully disperse in the oil, and the base oil enters the interlayer of the STAB-ZrP. In the STAB-ZrP gel system, STAB-ZrP and the base oil form a collective stable colloidal system. STAB-ZrP as a new thickener can thicken the five types of base oils with features characteristic of grease. Naphthenic and alkyl naphthalene oil had higher thickening ability, and this thickening law was similar to lithium-based grease [7–9]. The viscoelasticity and fluidity behavior of the STAB-ZrP gels were consistent with those of their base oils. The friction test showed that STAB-ZrP gels have excellent anti-wear and friction-reduction properties. In the STAB-ZrP gel system, STAB-ZrP is not merely a thickener but also a good solid additive, with STAB-ZrP acting as both a thickener and an additive in gel systems.

This research systematically revealed the correlation between STAB-ZrP thickener and base oils, and established the relationship of STAB-ZrP with the type of base oil in terms of performance. Herein, STAB-ZrP acts as a thickener and solid additive with two roles in the STAB-ZrP gel system. Although STAB-ZrP

gel still cannot meet the requirements of practical applications, due to the limited studies, this thickener design provides a new development idea for future grease preparations.

4 Conclusion

In this paper, STAB-ZrP intercalation samples were prepared by direct hydrothermal synthesis, and gels were prepared by thickening five types of base oils with STAB-ZrP. The conclusions are summarized as follows:

After the thickening process, the XRD results showed that all the obtained STAB-ZrP samples kept their original layered crystal structure. The interlayer spacing with PAO, POE, AN, and S8 as the base oil clearly shifted forward. The morphology of STAB-ZrP powder was no longer aggregated, forming cavities of different sizes. These results indicated that the base oil had entered the STAB-ZrP interlayer.

As a thickener, STAB-ZrP thickened the five types of base oil. AN oil and KN4010 oil had the best thickening ability among the five types of oil. PAO oil was better than S8 oil and POE oil. Naphthenic and aromatic hydrocarbons in the base oil increased the thickening ability of the STAB-ZrP gel. The STAB-ZrP gel samples resembled lubricating grease in appearance, and had the same color as their base oils.

Temperature affected the viscoelasticity and fluidity behavior of the gel. In all cases, the storage modulus value of STAB-ZrP gel at -15°C was higher than that at 25°C . KN4010G always maintained the most stable gel structure at 25°C and -15°C . The flow index values of PAOG and ANG showed small changes in amplitude. The colloidal stability of S8G and POEG worsened at low temperatures. The apparent viscosities of the five types of base oil and their STAB-ZrP gels increased as the temperature decreased.

STAB-ZrP gel not only ran smoothly during the whole process, but also had much lower wear volume and mean friction coefficient values than their base oils—except in the case of KN4010G, where a seizure occurred at -15°C due to high viscosity. The worn surfaces lubricated by STAB-ZrP gels were shallow and smooth. The EDS results indicated that STAB-ZrP adhered to the surface to form a protective film.

Taken together, our results demonstrate that STAB-ZrP is not only a thickener but also a solid lubricant. Our study can serve as a reference for the future development of grease preparation.

Declarations

Author Contribution

Jinxiang Dong: Conceptualization, methodology, investigation, supervision, funding acquisition. Hong Xu: methodology, writing—review and editing, funding acquisition. Yiling Wu: Methodology, Investigation, Writing—original draft. Zhiguo Hou: Methodology. Xinrui Zhao: Methodology. All authors reviewed the manuscript.

Data Availability

The data used in this research are available upon request.

References

1. Holmberg, K., Erdemir, A.: The impact of tribology on energy use and CO₂ emission globally and in combustion engine and electric cars. *Tribol. Int.* **135**, 389–396 (2019)
2. Ahmed, E., Nabhan, A., Ghazaly, N.M., Abdel-Jaber, G.J.S., Ltd, E.P.C.: Tribological Behavior of Adding Nano Oxides Materials to Lithium Grease: A Review
3. Lugt, P.M., Pallister, D.M.: Grease Lubrication in Rolling Bearings. *Grease Lubrication in Rolling Bearings* (2013)
4. Baily, W.W.: NLGI Spokesm. **45**, 261–265 (1990)
5. Materials, A.: S.f.T.a.: Standard Definitions of Terms Relating to Petroleum. Place (1959)
6. Waal, G.V.D., Kenbeek, D.J.: J.o.S.L. Testing, application, and future development of environmentally friendly ester base fluids. **10** (1993)
7. Porfiryev, Y., Shuvalov, S., Popov, P., Kolybelsky, D., Petrova, D., Ivanov, E., et al.: Effect of Base Oil Nature on the Operational Properties of Low-Temperature Greases. *ACS Omega*. **5**, 11946–11954 (2020)
8. Xu, N., Wang, X., Ma, R., Li, W., Zhang, M.: Insights into the rheological behaviors and tribological performances of lubricating grease: entangled structure of a fiber thickener and functional groups of a base oil. *New J. Chem.* **42**, 1484–1491 (2018)
9. Zhang, E., Li, W., Zhao, G., Wang, Z., Wang, X.: A Study on Microstructure, Friction and Rheology of Four Lithium Greases Formulated with Four Different Base Oils. *Tribol. Lett.* **69** (2021)
10. De Laurentis, N., Cann, P., Lugt, P.M., Kadiric, A.: The Influence of Base Oil Properties on the Friction Behaviour of Lithium Greases in Rolling/Sliding Concentrated Contacts. *Tribol. Lett.* **65** (2017)
11. Alberti, G., Costantino, U., Millini, R., Perego, G., Vivani, R.J.J.: J.o.S.S.C. Preparation, Characterization, and Structure of α -Zirconium Hydrogen Phosphate Hemihydrate. **113**:289–295 (1994)
12. Martín-Alfonso, J.E., Martín-Alfonso, M.J., Valencia, C., Cuberes, M.T.: Rheological and tribological approaches as a tool for the development of sustainable lubricating greases based on nano-montmorillonite and castor oil. *Friction*. **9**, 415–428 (2020)
13. Wang, Y., Zhang, P., Lin, J., Gao, X.: Rheological and Tribological Properties of Lithium Grease and Polyurea Grease with Different Consistencies. *Coatings* **12** (2022)
14. Garshin, M.V., Porfiryev, Y.V., Zaychenko, V.A., Shuvalov, S.A., Kolybelsky, D.S., Gushchin, P.A., et al.: Effect of Base Oil Composition on the Low-Temperature Properties of Polyurea Greases. *Pet. Chem.* **57**, 1177–1181 (2018)
15. Weijun, W.A.N.G., Yifeng, C.J.H.E., Hui, Z., Hongwei, S., YAO Lidan: Effect of mineral base oil on rheology of lithium base grease. *Acta Petrolei Sinica (Petroleum Processing Section)*. **34**(2), 316–

16. Fan, X.Q., Li, W., Li, H., Zhu, M.H., Xia, Y.Q., Wang, J.J.: Probing the effect of thickener on tribological properties of lubricating greases. *Tribol. Int.* **118**, 128–139 (2018)
17. Liu, L., Chen, Z.F., Wei, H.B., Li, Y., Fu, Y.C., Xu, H., et al.: Ionothermal synthesis of layered zirconium phosphates and their tribological properties in mineral oil. *Inorg. Chem.* **49**, 8270–8275 (2010)
18. Zhang, X., Xu, H., Zuo, Z., Lin, Z., Ferdov, S., Dong, J.: Hydrothermal synthesis of copper zirconium phosphate hydrate [Cu(OH)2Zr(HPO4)2.2H2O] and an investigation of its lubrication properties in grease. *ACS Appl. Mater. Interfaces.* **5**, 7989–7994 (2013)
19. Niu, W., Liu, L., Xu, H., Dong, J.: Tribological properties of zirconium phosphate-quinoline compound as an additive in lithium grease. *Industrial Lubrication and Tribology.* **70**, 1487–1493 (2018)
20. Han, X., Yong, H., Sun, D.: Tuning Tribological Performance of Layered Zirconium Phosphate Nanoplatelets in Oil by Surface and Interlayer Modifications. *Nanoscale Res. Lett.* **12**, 542 (2017)
21. Jiang, F., Sun, H., Chen, L., Lei, F., Sun, D.: Dispersion-tribological property relationship in mineral oils containing 2D layered α -zirconium phosphate nanoplatelets. *Friction.* **8**, 695–707 (2019)

Figures

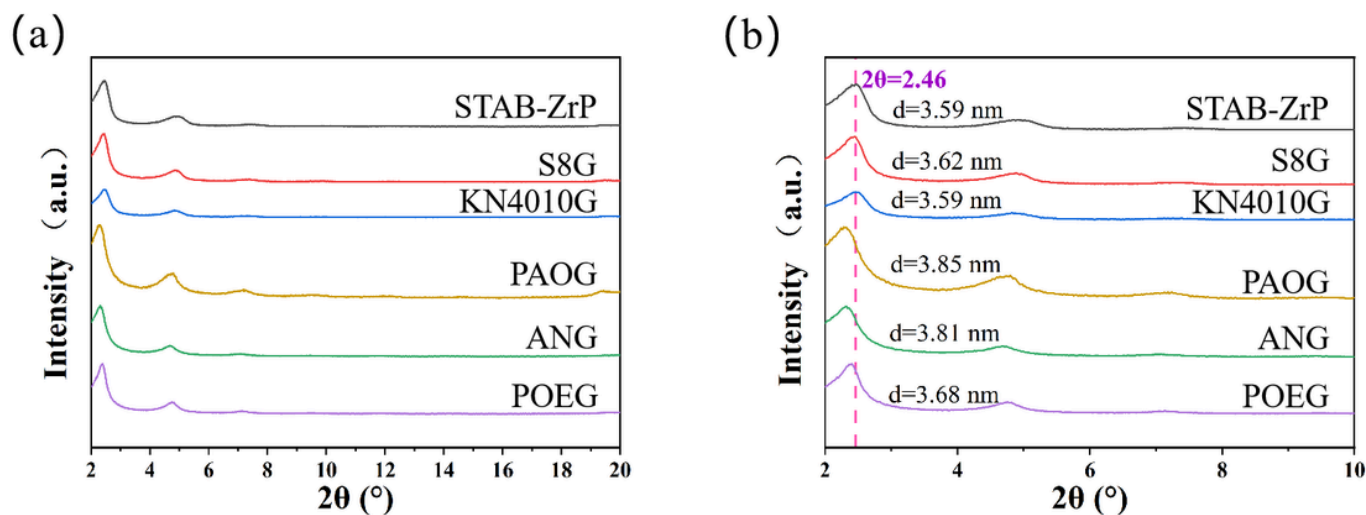


Figure 1

XRD spectra of STAB-ZrP and STAB-ZrP gel samples with five types of base oils: **a** overall pattern ($2\theta = 2^\circ - 20^\circ$) and **b** zoomed-in pattern ($2\theta = 2^\circ - 10^\circ$)

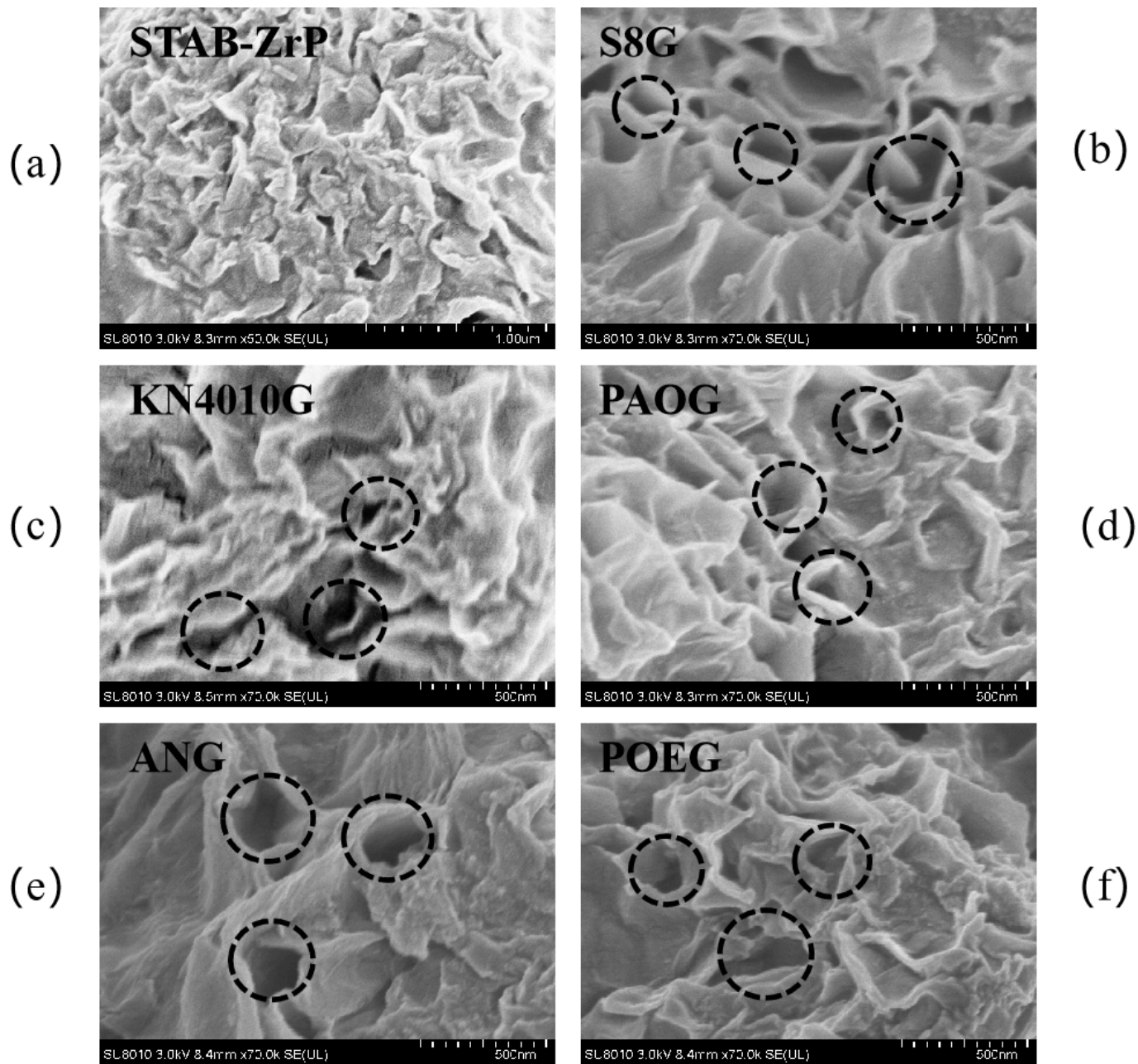


Figure 2

SEM morphology of STAB-ZrP and STAB-ZrP gel samples with five base oils: **a** STAB-ZrP, **b** S8G, **c** KN4010G, **d** PAOG, **e** ANG, and **f** POEG

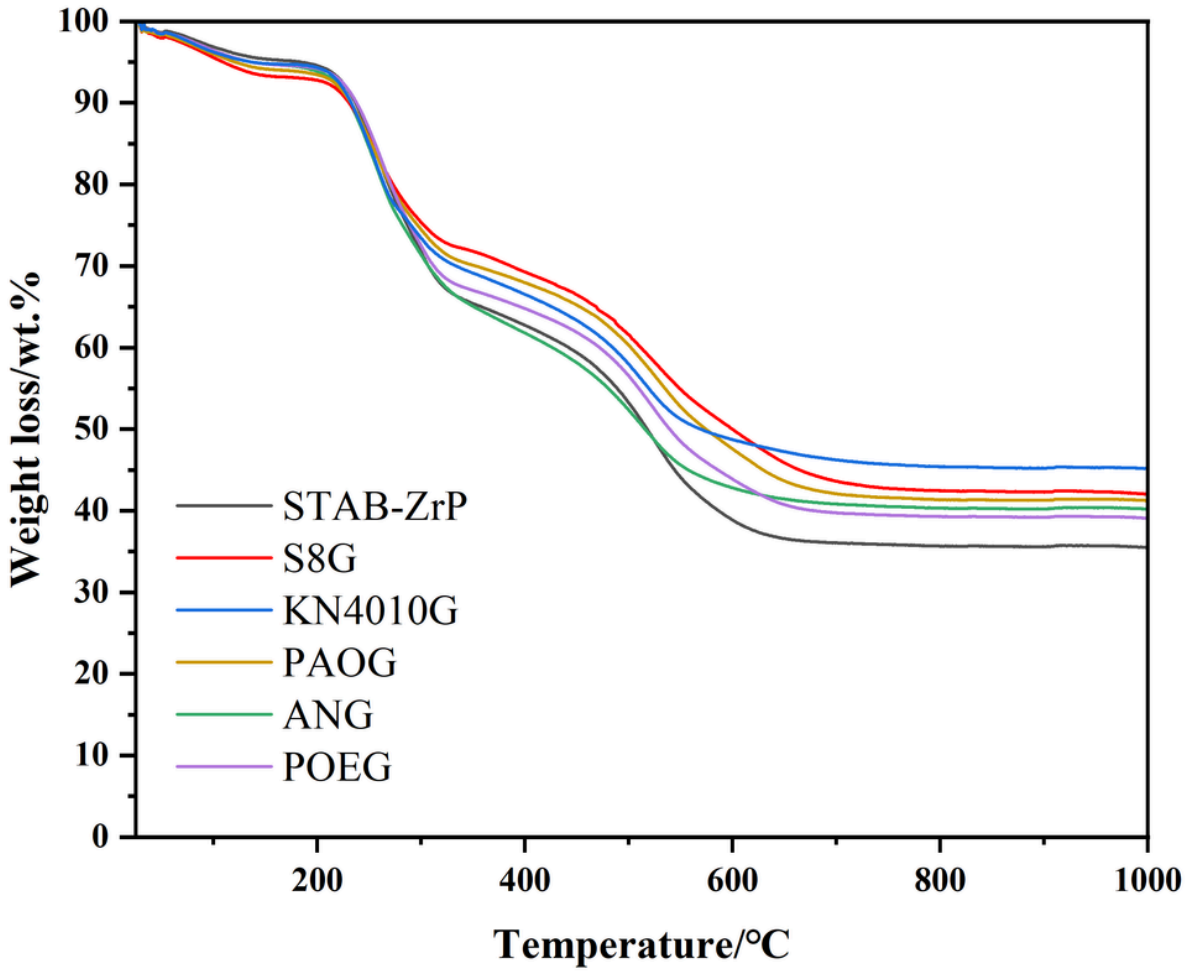


Figure 3

TG curves of STAB-ZrP and STAB-ZrP gel samples with the five base oils

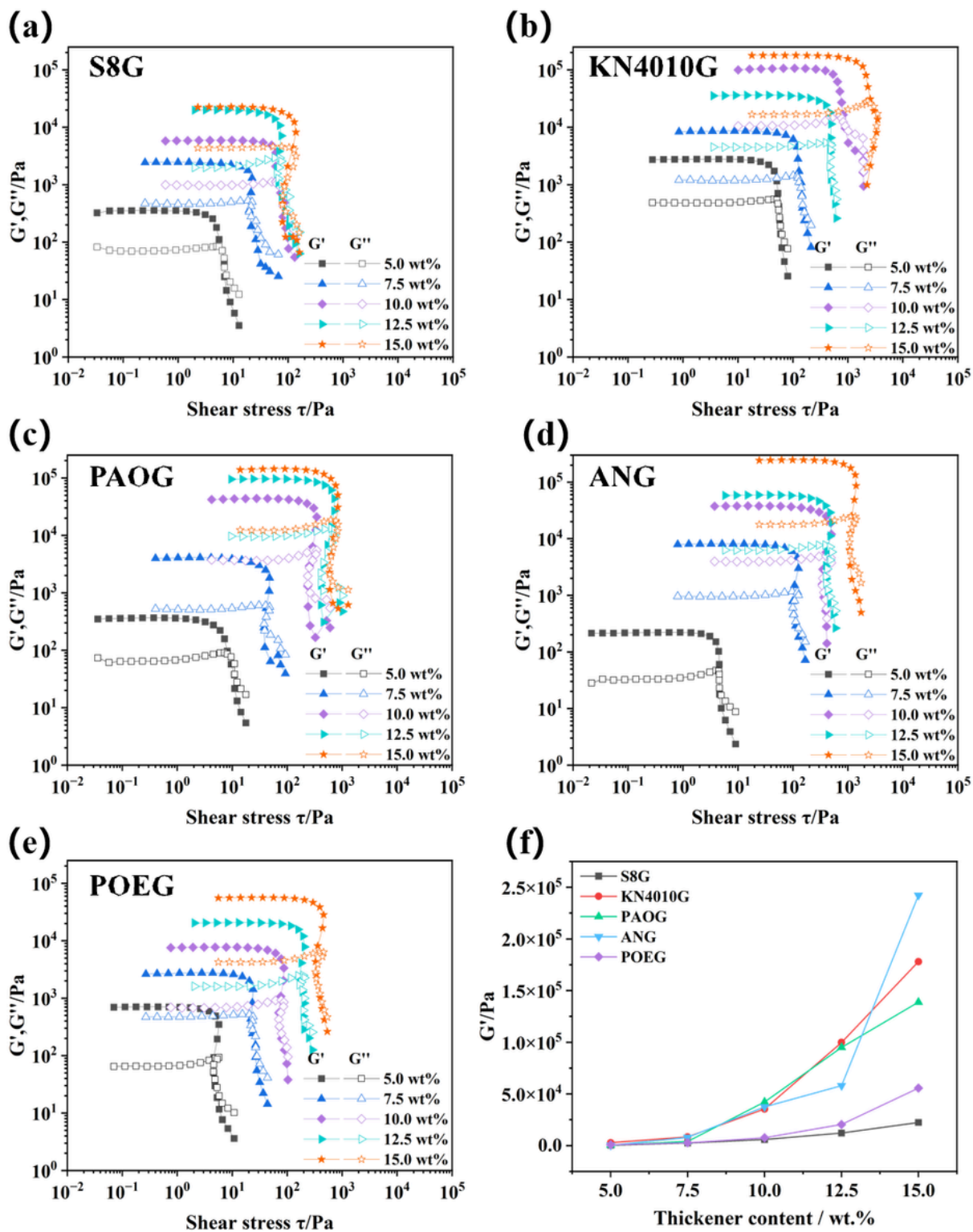


Figure 4

Viscoelasticity behavior of STAB-ZrP gel as the function of different STAB-ZrP content: **a** S8G, **b** KN4010G, **c** PAOG, **d** ANG, **e** POEG, and **f** the storage modulus of STAB-ZrP gel with the five base oils at different STAB-ZrP concentrations

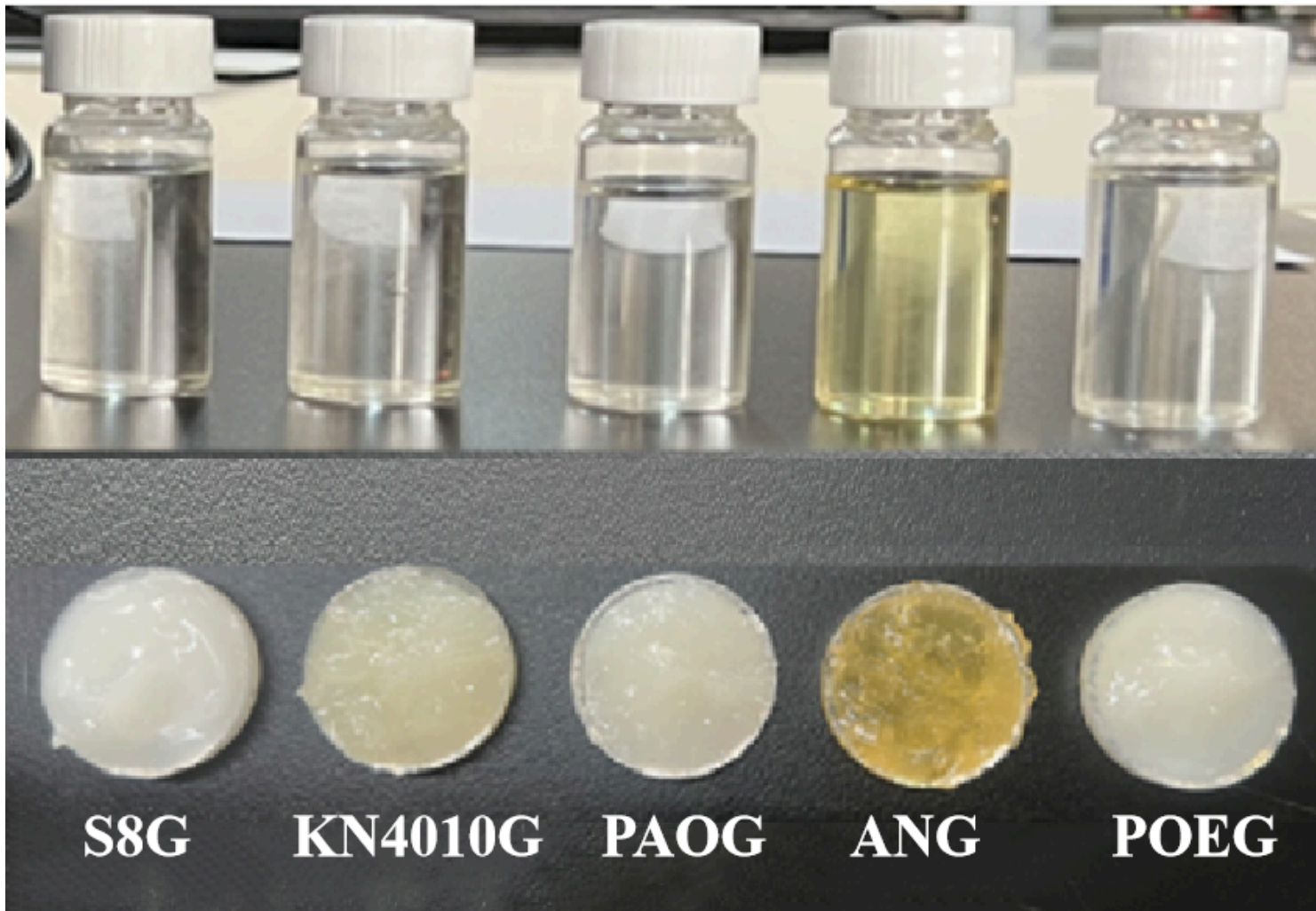


Figure 5

Photographs of the five base oils and their 10.0 wt.% STAB-ZrP gel samples

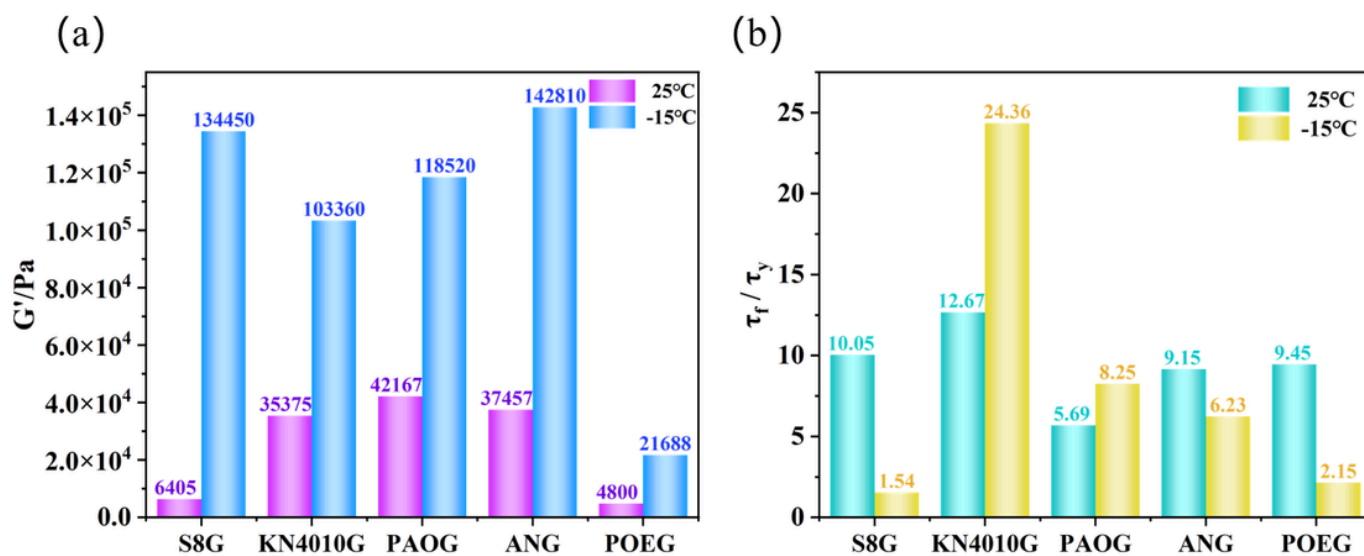


Figure 6

Viscoelasticity and fluidity behavior of the STAB-ZrP gel as a function of temperature: **a** the storage modulus behavior of the STAB-ZrP gel, **b** the fluidity behavior of the STAB-ZrP gel

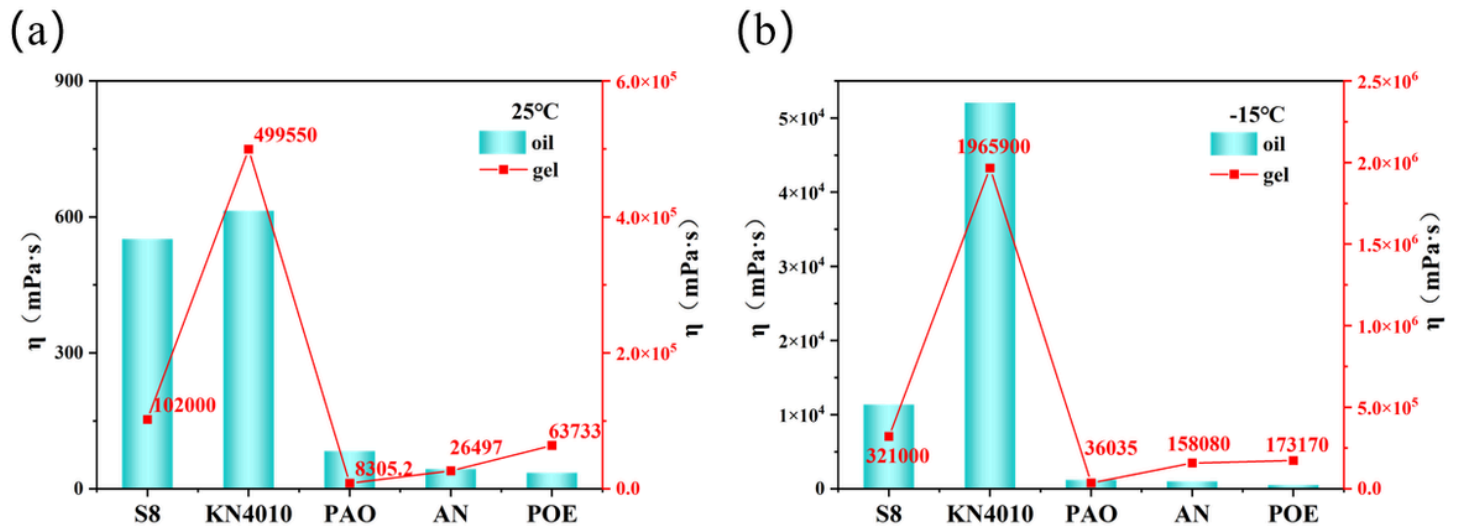
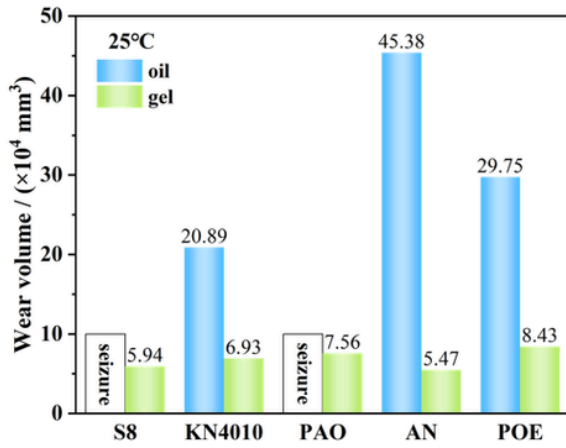


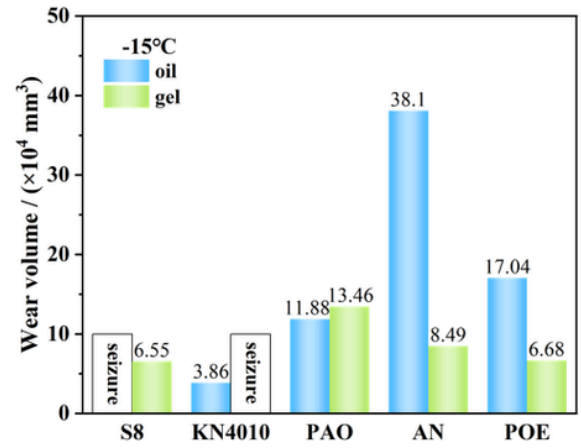
Figure 7

Apparent viscosity–temperature relationship of the five base oils and their STAB-ZrP gels: **a** 25°C, **b** -15°C

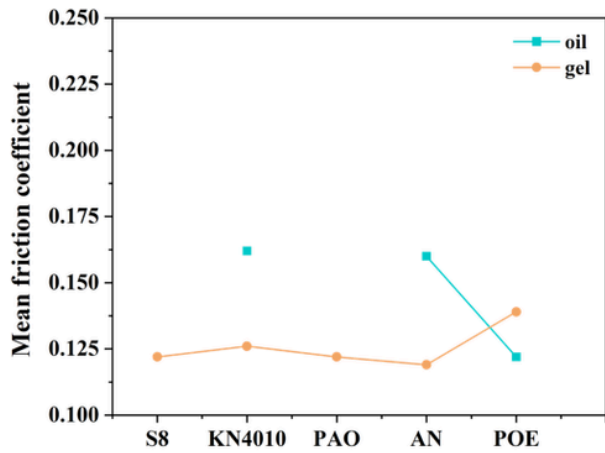
(a)



(b)



(c)



(d)

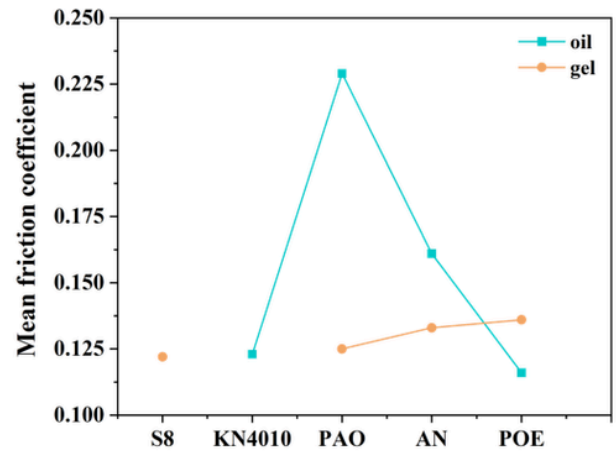


Figure 8

Wear volume and mean friction coefficients of the five base oils and their STAB-ZrP gels: **a** and **c** 25°C, **b** and **d** -15°C (SRV tester, load 200 N, frequency 50 Hz, time 2 h)

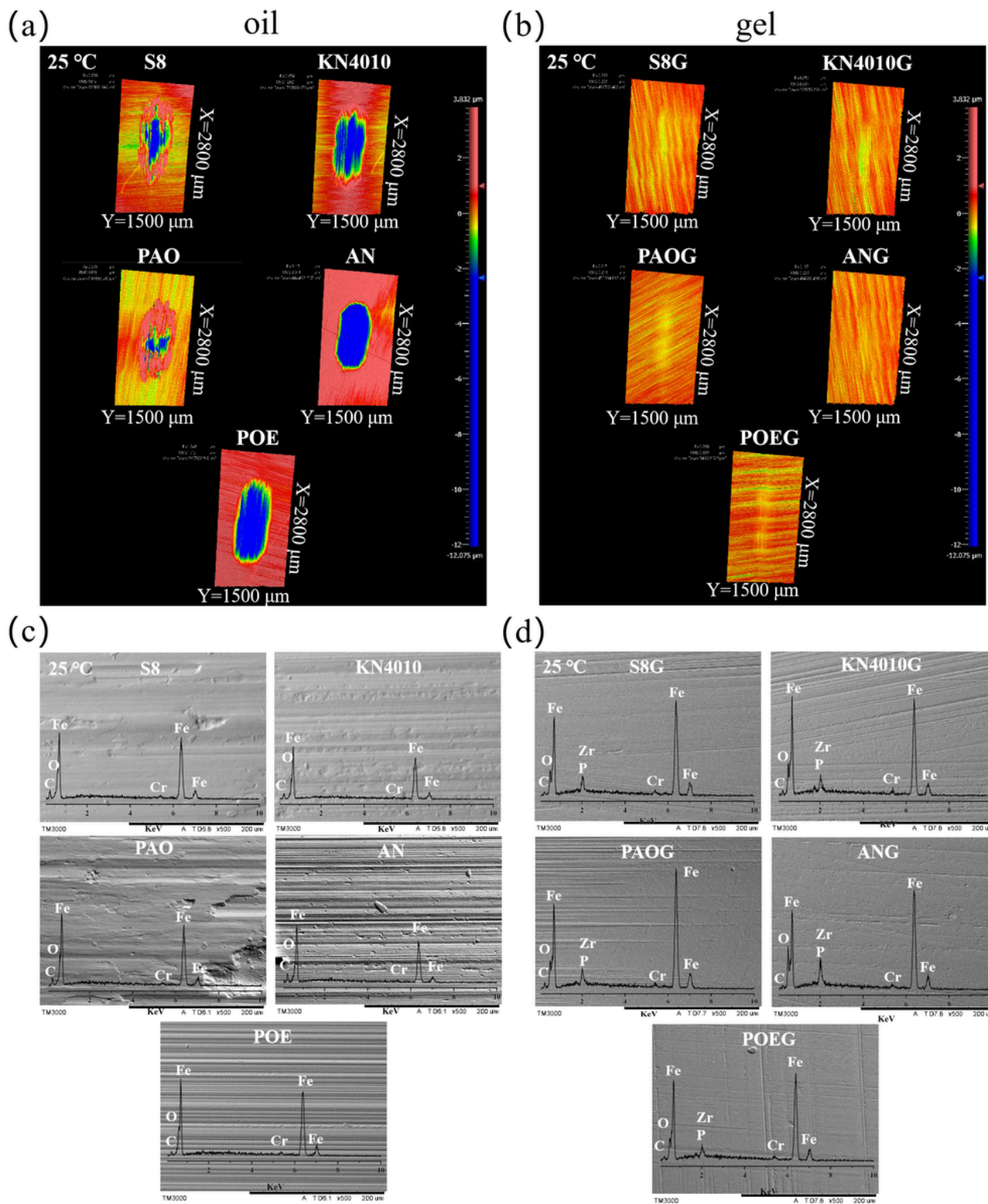


Figure 9

3D morphology, SEM morphology, and EDS elemental distribution of steel disks lubricated by the five base oils and their STAB-ZrP gels: **a** and **c** five base oils, **b** and **d** STAB-ZrP gels (SRV tester, load 200 N, frequency 50 Hz, time 2 h, temperature 25 °C)

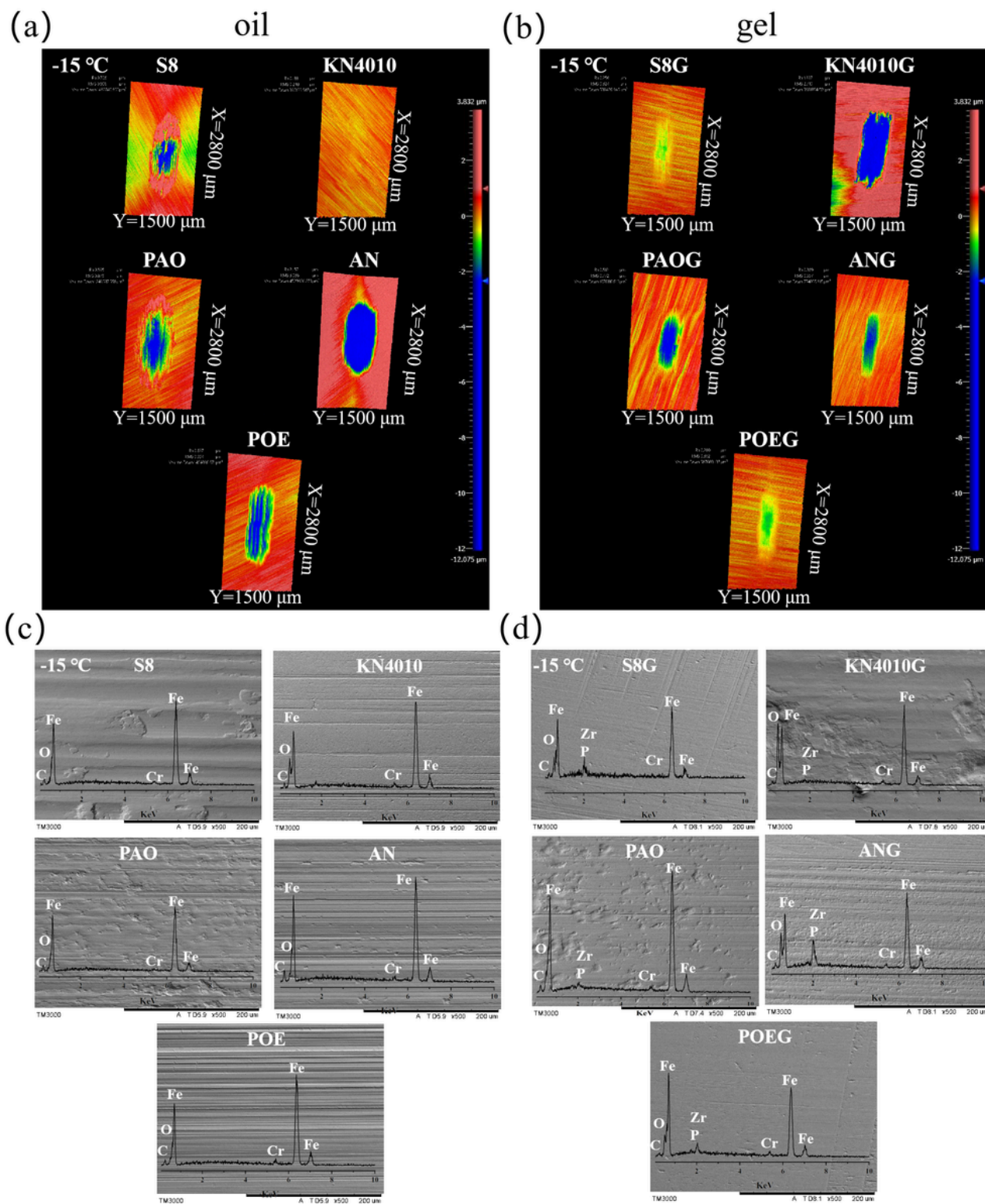


Figure 10

3D morphology, SEM morphology, and EDS elemental distribution of steel disks lubricated by the five base oils and their STAB-ZrP gels: **a** and **c** five base oils, **b** and **d** STAB-ZrP gels (SRV tester, load 200 N, frequency 50 Hz, time 2 h, temperature -15°C)

Supplementary Files

This is a list of supplementary files associated with this preprint. Click to download.

- [Highlights.docx](#)
- [Supplementarymaterial.docx](#)
- [GraphicalAbstact.tif](#)